© The American Society of Gene & Cell Therapy

The Extracellular Matrix Glycoprotein Tenascin-C Is Beneficial for Spinal Cord Regeneration

Jian Chen[1], Hyun Joon Lee[2], Igor Jakovcevski[2], Ronak Shah[1], Neha Bhagat[1], Gabriele Loers[2], Hsing-Yin Liu[3], Sally Meiners[3], Grit Taschenberger[4], Sebastian Kügler[4], Andrey Irintchev[2,5] and Melitta Schachner[1,2]

[1]W.M. Keck Center for Collaborative Neuroscience, Department of Cell Biology and Neuroscience, Rutgers the State University of New Jersey, Piscataway, New Jersey, USA; [2]Zentrum für Molekulare Neurobiologie, University Hospital Hamburg-Eppendorf, Universität Hamburg, Hamburg, Germany; [3]UMDNJ-Robert Wood Johnson Medical School, Department of Pharmacology, Piscataway, New Jersey, USA; [4]DFG Research Center Molecular Physiology of the Brain (CMPB) at Department of Neurology, University of Goettingen, Goettingen, Germany; [5]Department of Otorhinolaryngology, Friedrich-Schiller-University Jena, Jena, Germany

Tenascin-C (TNC), a major component of the extracellular matrix, is strongly upregulated after injuries of the central nervous system (CNS) but its role in tissue repair is not understood. Both regeneration promoting and inhibiting roles of TNC have been proposed considering its abilities to both support and restrict neurite outgrowth *in vitro*. Here, we show that spontaneous recovery of locomotor functions after spinal cord injury is impaired in adult TNC-deficient ($TNC^{-/-}$) mice in comparison to wild-type ($TNC^{+/+}$) mice. The impaired recovery was associated with attenuated excitability of the plantar Hoffmann reflex (H-reflex), reduced glutamatergic input, reduced sprouting of monaminergic axons in the lumbar spinal cord and enhanced post-traumatic degeneration of corticospinal axons. The degeneration of corticospinal axons in $TNC^{-/-}$ mice was normalized to $TNC^{+/+}$ levels by application of the alternatively spliced TNC fibronectin type III homologous domain D (fnD). Finally, overexpression of TNC-fnD *via* adeno-associated virus in wild-type mice improved locomotor recovery, increased monaminergic axons sprouting, and reduced lesion scar volume after spinal cord injury. The functional efficacy of the viral-mediated TNC indicates a potentially useful approach for treatment of spinal cord injury.

Received 20 May 2010; accepted 28 May 2010; published online 6 July 2010. doi:10.1038/mt.2010.133

INTRODUCTION

Lack of regeneration in the mature central nervous system (CNS) of mammals is attributed to the prevalence of neurite outgrowth inhibitory over conducive molecules. Several CNS myelin-associated inhibitors have been identified and characterized: Nogo-A,[1] myelin-associated glycoprotein,[2] oligodendrocyte myelin glycoprotein,[3] semaphorin 3A,[4] chondroitin sulfate proteoglycans,[5] and tenascin-R.[6] Enzymatic degradation of the chondroitin sulfate moiety of chondroitin sulfate proteoglycans improves axon regeneration[7] after spinal cord injury in adult rats, indicating a prominent role of these extracellular matrix constituents in preventing axonal regeneration.

A major component of the extracellular matrix is the glycoprotein tenascin-C (TNC), which is expressed by mature and immature astrocytes, radial glia, meningeal fibroblasts, subsets of neurons, and Schwann cells.[8–11] TNC expression is upregulated by glial cells following CNS trauma,[10] as well as by neurons after exposure to excitotoxic agents or induction of long-term potentiation.[12,13] TNC has been implicated not only in enhancement of neurite outgrowth and polarity of some neurons *in vitro*, but also in inhibition of other neuronal cell types.[14–16] TNC inhibits outgrowth when offered as a sharp substrate boundary abutting onto a neurite outgrowth conducive environment.[17] These dual properties have been assigned to different splice variants of TNC[18] and molecular epitopes within those splice variants.[14,16,19–23]

Little is known about the *in vivo* functional role of TNC after CNS lesions. In this study, we studied a TNC-deficient mouse, which has normal gross anatomy of the CNS.[24] We found that compression lesion of the spinal cord of adult mice leads to reduced functional outcome, and a more pronounced dying back of severed corticospinal axons in $TNC^{-/-}$ compared to $TNC^{+/+}$ mice. This axonal retraction was reduced by application of the alternatively spliced fibronectin type III homologous domain D (fnD) to the injured spinal cord of $TNC^{-/-}$ mice. Overexpression of fnD by an adeno-associated viral (AAV) vector promoted the locomotor functional and morphological recovery in wild-type mice after compression spinal cord injury. These results indicate that TNC promotes spinal cord regeneration.

RESULTS

Locomotor recovery of $TNC^{-/-}$ mice is inferior to that of $TNC^{+/+}$ littermates after spinal cord injury

To evaluate the role of TNC in regeneration after spinal cord injury, we first compared locomotor recovery after compression injury between $TNC^{-/-}$ and $TNC^{+/+}$ mice using the Basso Mouse Score (BMS) rating scale[25] and an objective numerical measure of the plantar stepping abilities, the foot-stepping angle during beam walking.[6] Locomotor performance of $TNC^{-/-}$ mice

The first two authors contributed equally to this work.

Correspondence: *Melitta Schachner, W.M. Keck Center, 604 Allison Road, Piscataway, New Jersey 08854, USA. E-mail: schachner@biology.rutgers.edu*

© The American Society of Gene & Cell Therapy

before injury was similar to that of $TNC^{+/+}$ mice (Figure 1), in agreement with previous observations that $TNC^{-/-}$ mice have no apparent motor deficits.[26] One week after compression injury, both $TNC^{+/+}$ and $TNC^{-/-}$ mice had a severe decline in the BMS score and a prominent increase in the foot-stepping angle (Figure 1a,b). During the 12-week observation period, locomotor abilities recovered to a moderate degree in both genotypes, but this recovery was more impaired in $TNC^{-/-}$ mice in comparison to their $TNC^{+/+}$ littermates (Figure 1). Group mean values differed statistically only for the BMS score 12 weeks after injury (Figure 1a). However, analysis of recovery indexes, which estimate gain of function after the first week as a fraction of the functional loss induced by the injury in individual animals,[6] revealed significant differences for both parameters at 6 and 12 weeks after injury (Figure 1c,d). These results indicate an adverse effect of TNC ablation on hindlimb locomotion after spinal cord injury.

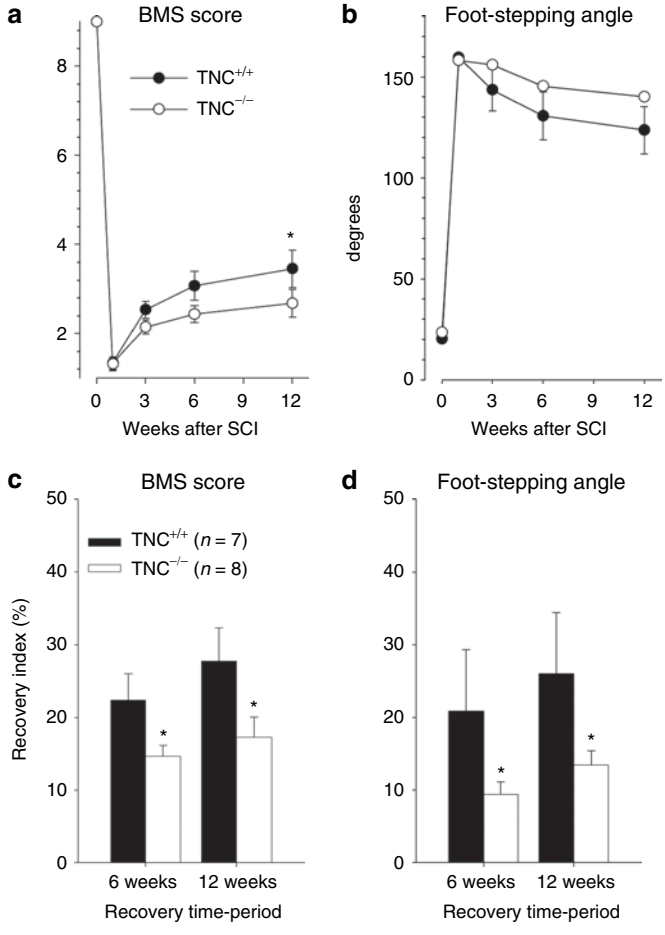

Figure 1 Functional recovery after compression spinal cord injury in $TNC^{-/-}$ and $TNC^{+/+}$ mice estimated by Basso Mouse Score (BMS) rating and foot-stepping angle. Mean values (±SEM) of (**a**) BMS scores and (**b**) foot-stepping angles before surgery (day 0) and at 1, 3, 6, and 12 weeks after injury. Recovery indexes (mean values ± SEM) calculated from individual animal values for (**c**) BMS score and (**d**) foot-stepping angle at 6 and 12 weeks after injury. Numbers of animals per group are indicated in **c**. Asterisks indicate significant differences between group mean values at a given time period (one-way analysis of variance for repeated measurements with Tukey's *post hoc* test, $P < 0.05$). TNC, tenascin-C.

Reduced H-reflex activity in $TNC^{-/-}$ mice versus $TNC^{+/+}$ littermates after spinal cord injury

In addition to assessment of locomotor recovery, we analyzed the plantar H-reflex (Hoffmann reflex), an electrically elicited analog of the spinal stretch reflex providing information about the functional properties of Ia afferents and homonymous α-motoneurons. Before injury, the H-reflex responses were strongly reduced in both $TNC^{-/-}$ and $TNC^{+/+}$ mice when the stimulation frequency was increased stepwise from baseline frequency (0.1 Hz) to 5 Hz, a phenomenon known as rate depression (Figure 2). One week after injury, the rate depression was severely reduced in both genotypes (Figure 2). At later time points, 3–12 weeks, the rate sensitivity declined further, as compared with 1 week, in $TNC^{+/+}$ mice, but not in $TNC^{-/-}$ mice (Figure 2). Thus, reflex excitability upon repetitive stimulation was significantly reduced in $TNC^{-/-}$ mice compared with $TNC^{+/+}$ littermates at 6 and 12 weeks, which is consistent with previous locomotor recovery observations. Previous work in rats and mice has shown that reduced reflex excitability is associated with reduced locomotor recovery.[27] Thus, our combined observations suggest that TNC deficiency prevents functionally favorable changes in reflex excitability with time after injury. In contrast to $TNC^{-/-}$ mice, mice deficient in tenascin-R, a TNC-related extracellular matrix molecule, show both improved locomotor recovery and enhanced reflex excitability compared with wild-type littermates after compression spinal cord injury.[6,27]

Reduced afferent input to lamina VII in $TNC^{-/-}$ mice versus $TNC^{+/+}$ littermates after spinal cord injury

The degree of locomotor recovery after spinal cord injury is largely determined by preservation and functionality of primary afferent inputs.[28] We therefore investigate, whether some aspects of spinal cord connectivity are altered in $TNC^{-/-}$ mice. We analyzed vesicular glutamate transporter 1 $(VGLUT1)^+$ synaptic terminals, which are derived from medium- to large-sized neurons in the dorsal root ganglia and convey mechano- and proprioceptive information to the spinal cord.[29] We selected three areas for analysis in which $VGLUT1^+$ terminal densities were prominent: the Clarke's column, which receives proprioceptive information (Figure 3a,b), an adjacent part of lamina VII, an area in the spinal cord containing, among

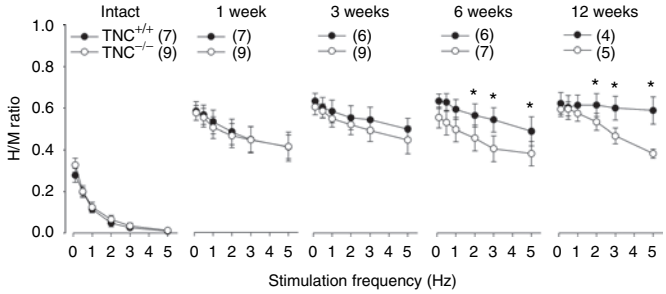

Figure 2 Rate depression of the Hoffmann reflex at different time points after spinal cord injury in $TNC^{-/-}$ and $TNC^{+/+}$ mice. Shown are mean values (±SEM) of H/M ratios at different stimulation frequencies before operation and 1, 3, 6, and 12 weeks after spinal cord injury. At 6 and 12 weeks after injury, the H/M ratios in $TNC^{-/-}$ mice are significantly lower than in $TNC^{+/+}$ littermates at high frequencies (analysis of variance for repeated measurements with Tukey's *post hoc* test, $*P < 0.05$). Number of animals are indicated in parenthesis. TNC, tenascin-C.

© The American Society of Gene & Cell Therapy

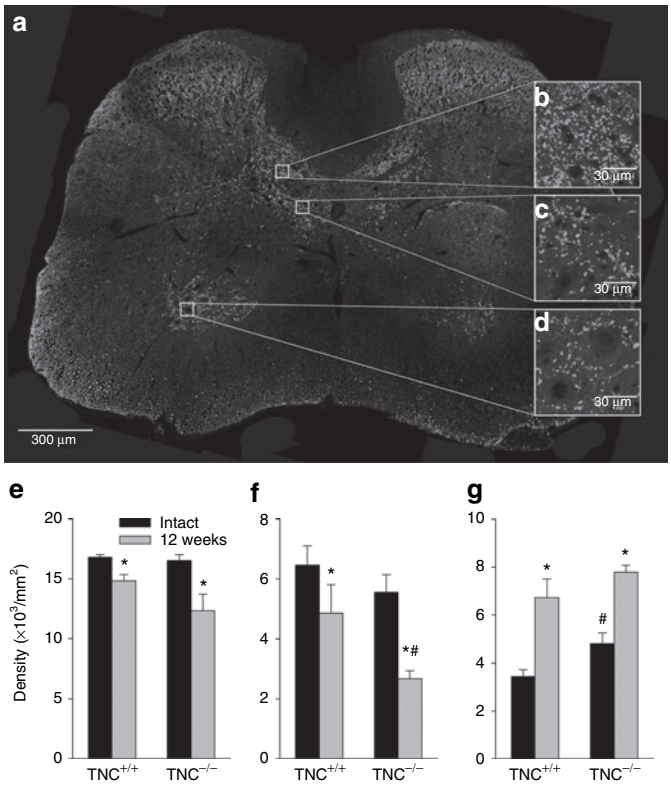

Figure 3 Immunohistochemical analysis of VGLUT1$^+$ terminals in the spinal cord of intact and injured TNC$^{-/-}$ and TNC$^{+/+}$ mice. (**a**) A representative section of the spinal cord of a TNC$^{+/+}$ mouse shows the distribution of VGLUT1$^+$ puncta. Digital images of VGLUT1$^+$ terminals in the (**b**) Clarke's column, (**c**) medial lamina VII, and (**d**) lamina IX obtained at high magnification (insets **b**, **c**, **d**) were used for estimation of terminal densities (number of puncta per unit area). Mean densities (±SEM) of terminals in the three areas in injured and intact TNC$^{-/-}$ (n = 5) and TNC$^{+/+}$ mice (n = 4) are shown in **e**–**g**. Six sections 250 µm apart were analyzed per animal. Asterisks indicate differences between noninjured and injured mice of the same genotype, cross-hatches denote differences between intact or injured TNC$^{-/-}$ and TNC$^{+/+}$ mice ($P < 0.05$, two-sided t-test for independent samples). TNC, tenascin-C; VGLUT1, vesicular glutamate transporter 1.

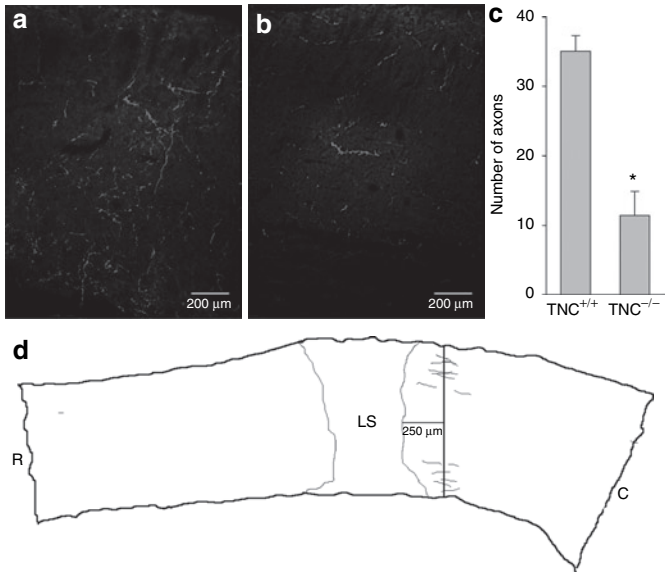

Figure 4 Analysis of monaminergic axons in the lumbar spinal cord of TNC$^{-/-}$ and TNC$^{+/+}$ mice 12 weeks after injury. Representative images of tyrosine hydroxylase-positive (TH$^+$) fibers in (**a**) TNC$^{+/+}$ and (**b**) TNC$^{-/-}$ mice. (**c**) Mean numbers (±SEM) of TH$^+$ axons in four TNC$^{+/+}$ and three TNC$^{-/-}$ mice. Every 5th parasagittal serial section from the spinal cord of each animal was analyzed. (**d**) The axon counting paradigm is illustrated in the Neurolucida drawing. Asterisk indicates significant difference between TNC$^{-/-}$ and TNC$^{+/+}$ mice ($P < 0.05$, two-sided t-test for independent samples). C, caudal; LS, lesion site; R, rostral; TNC, tenascin-C.

other neurons, last-order interneurons, *i.e.*, innervating motoneurons (Figure 3a,c) and the motoneuron region, lamina IX, where proprio- and mechanoreceptors form contacts predominantly on motoneuron dendrites (Figure 3a,d). Analysis of TNC$^{+/+}$ mice 12 weeks after injury revealed a significant, compared with noninjured mice, decline in the terminal densities in Clarke's column and lamina VII, and, interestingly, a strong increase in lamina IX (Figure 3e–g). Similar injury-related changes were found in TNC$^{-/-}$ mice with one prominent exception: a severe reduction of VGLUT1$^+$ boutons in lamina VII compared with both noninjured TNC$^{-/-}$ mice and injured TNC$^{+/+}$ mice (Figure 3f). This genotype-related difference indicates that TNC ablation leads to area-specific deficits in afferent inputs to the injured spinal cord.

Reduced regrowth/sprouting of monaminergic and CST axons in TNC$^{-/-}$ versus TNC$^{+/+}$ littermates after spinal cord injury

The deficit in the glutamatergic innervation of lamina VII in TNC$^{-/-}$ mice suggested that absence of TNC in the injured spinal cord has a negative impact on axonal survival and/or sprouting. To further analyze this possibility, we examined monaminergic (tyrosine hydroxylase-positive, TH$^+$) axons in the lumbar spinal cord. These axons often survive after thoracic compression or contusion injuries and are able to regrow and sprout.[30] In support of this view, we found a dramatic deficit in TH$^+$ axonal innervation of the lumbar spinal cord of injured TNC$^{-/-}$ mice compared with TNC$^{+/+}$ mice (Figure 4). Considering that the degree of monaminergic innervation of the lumbar spinal cord is an important determinant of locomotor abilities after spinal cord injury in rats and mice,[31–33] we conclude that the observed axonal deficit accounts, at least in part, for the inferior functional recovery in TNC$^{-/-}$ mice.

In addition to unmyelinated monaminergic fibers, we examined corticospinal tract (CST) axons to evaluate the response of large myelinated axons to spinal cord injury. The proximal segments of these axons degenerate rapidly, within hours after injury, and thus retract from the lesion site by several hundred micrometers.[34,35] We analyzed this "dying back" by measuring the distance between the tips of the anterogradely fluoro-ruby-labeled axons and the center of the lesion site (Figure 5). In TNC$^{+/+}$ mice, this distance was about 400 µm at 1 week after injury, and it did not change at 2 weeks as well as 30 days after injury. Similar retraction was found at 1 and 2 weeks after injury in TNC$^{-/-}$ mice. At 30 days, however, the distance in TNC$^{-/-}$ was more than doubled compared with the previous time points. Thus, TNC deficiency leads to a delayed secondary axonal degeneration. Combined, our findings support the

© The American Society of Gene & Cell Therapy

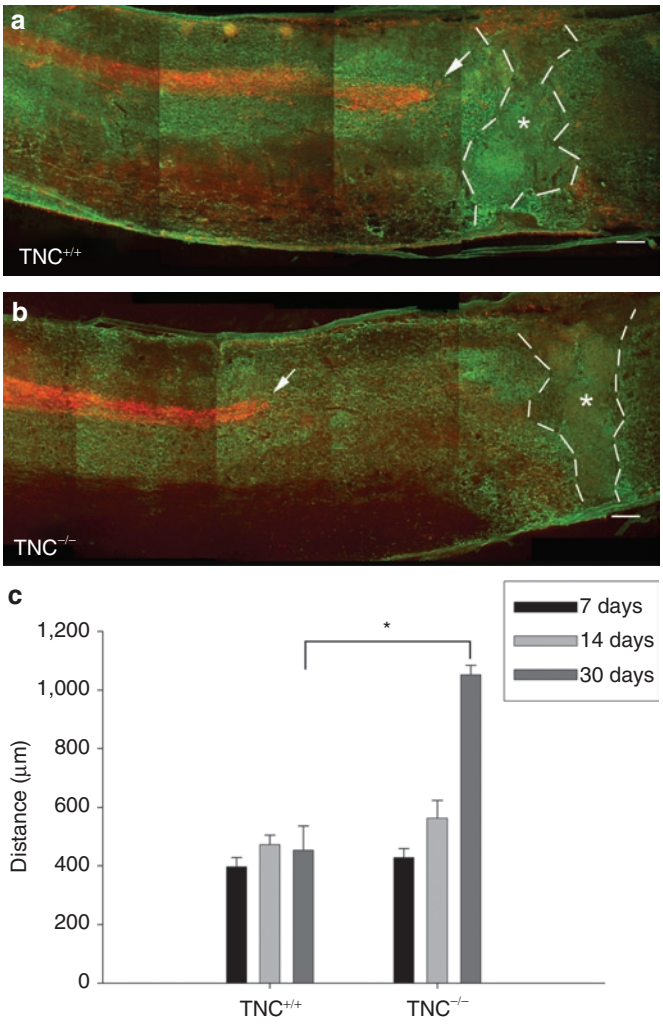

Figure 5 Corticospinal tract axonal 'dying-back' is reduced in TNC$^{-/-}$ mice after spinal cord injury. Localization of corticospinal tract axons anterogradely labeled with fluoro-ruby (red) with respect to the center of the lesion (indicated by stars) as seen by immunolabeling of astrocytes by GFAP (green) in consecutive longitudinal sections of a **(a)** TNC$^{+/+}$ and **(b)** TNC$^{-/-}$ mice 30 days after spinal cord injury. Tips of the longest axons of the corticospinal tracts are indicated by arrows. Bar = 100 µm. (**c**) Mean distances (±SEM) between the tips of the corticospinal tract axons and the lesion center in TNC$^{-/-}$ mice and TNC$^{+/+}$ mice at 7, 14, and 30 days after injury (n = 4 for each time point). Broken lines indicate extent of the glial scar. Asterisk indicates a significant difference between the genotypes ($P < 0.01$, t-test). GFAP, glial fibrillary acidic protein; TNC, tenascin-C.

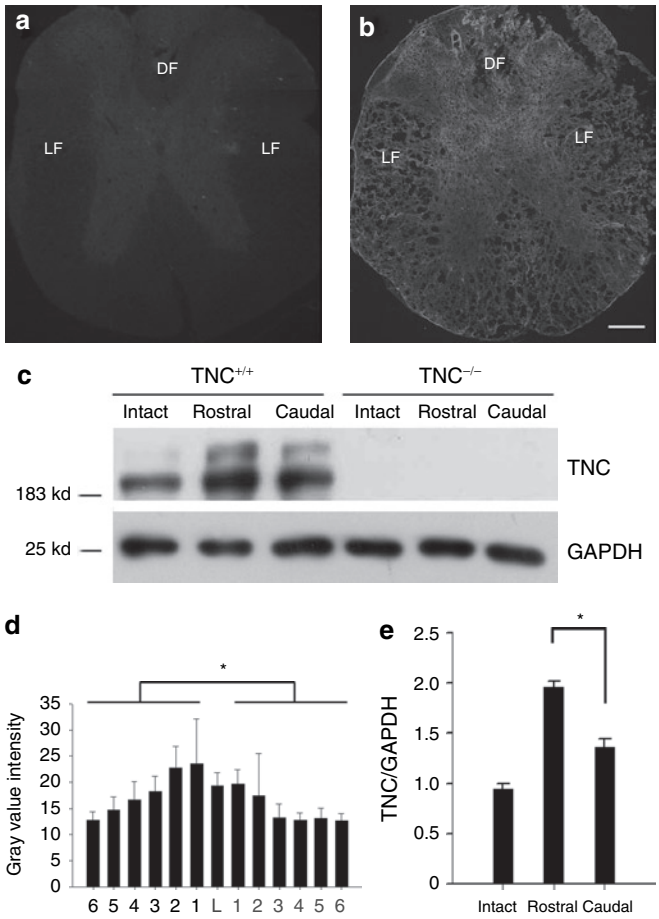

Figure 6 Immunohistochemical and western blot analysis of TNC expression in intact and injured spinal cords 4 days after injury. (**a**) By immunohistochemistry, TNC is hardly detectable in the intact spinal cord. (**b**) In the lesioned spinal cords of TNC$^{+/+}$ mice, 4 days after injury, TNC is upregulated in both gray matter and white matter. (**c**) Western blot analysis of TNC expression is consistent with the fluorescence intensity evaluation (n = 4 for western blot), with TNC being more predominantly expressed in the spinal cord rostral to the lesion site, less in the spinal cord caudal to the lesion site, and least in the intact spinal cord. Equal loading of protein extracts is seen by western blot analysis of GAPDH. (**d**) Mean immunofluorescence intensities in consecutive transverse spinal cord sections show higher levels of TNC in the spinal cord rostral than caudal to the lesion site (n = 4 for immunofluorescence, mean values ± SEM are shown). The lesion center is designated as level "L," and other sequential levels are designated as levels 1, 2, etc. at 600-µm spaced intervals rostrally and caudally from the lesion. (**e**) Quantitative evaluation of band intensities by western blot analysis of intact spinal cords and segments of injured spinal cords proximal and distal to the lesion site. Asterisk indicates a significant difference between groups ($P < 0.01$, t-test). Bar = 100 µm. DF, dorsal funiculus; GAPDH, glyceraldehyde-3-phosphate dehydrogenase; LF, lateral funiculus; TNC, tenascin-C.

notion that lack of TNC renders the hostile environment in the injured spinal cord even more unfavorable for axonal survival and regrowth.

TNC expression in the injured spinal cord of TNC$^{+/+}$ mice

We further analyzed the expression pattern of TNC in the injured spinal cord of wild-type mice by immunohistochemistry rostral and caudal to the lesion site as a function of time after lesion. In noninjured TNC$^{+/+}$ mice (Figure 6a) and in lesioned TNC$^{-/-}$ mice (data not shown), no TNC immunoreactivity was detected. In injured TNC$^{+/+}$ mice, TNC was upregulated already 2 days after injury rostral and caudal to the lesion site, reached a peak between 4 and 7 days after injury to be reduced thereafter, but still being elevated when compared to the uninjured spinal cords at 30 days (Figure 6b). To quantify TNC expression, digital images taken from serial sections were subjected to mean gray value detection as a measure of average fluorescence intensity. Significantly stronger TNC immunoreactivity was found rostral (125 ± 6.0 arbitrary units, AU) than

© The American Society of Gene & Cell Therapy

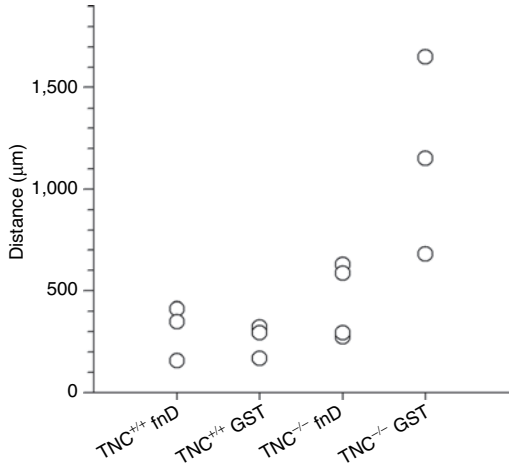

Figure 7 TNC-derived fusion protein GST-fnD rescues the dying back of corticospinal tract axons in TNC$^{-/-}$ mice but does not promote further regrowth of corticospinal tract axons in TNC$^{+/+}$ mice. The distance between the tips of the corticospinal tract axons and lesion center was used as index of axonal degeneration after spinal cord injury in individual animals (indicated by circles). Four groups were tested: TNC-derived fusion protein GST-fnD was administered to the spinal cords of TNC$^{+/+}$ (TNC$^{+/+}$ fnD, $n = 3$) and TNC$^{-/-}$ (TNC$^{-/-}$ fnD, $n = 4$) mice; similarly, GST was administered as control to TNC$^{+/+}$ (TNC$^{+/+}$ GST, $n = 3$) and TNC$^{-/-}$ (TNC$^{-/-}$ GST, $n = 3$) mice. fnD, fibronectin type III homologous domain D; GST, glutathione *S*-transferase; TNC, tenascin-C.

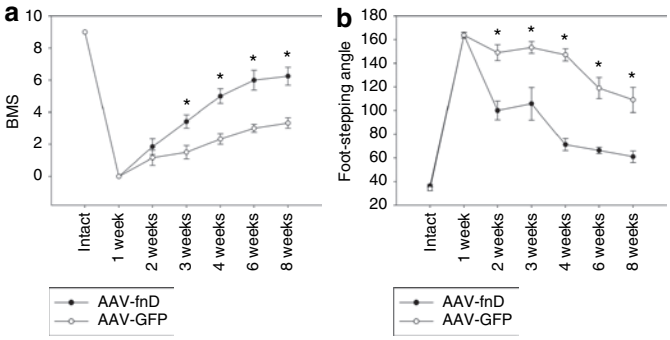

Figure 8 AAV-fnD improves locomotor recovery after spinal cord injury. Recovery was evaluated by (**a**) BMS and (**b**) foot-stepping angle at 1, 2, 3, 4, 6, and 8 weeks after spinal cord injury and AAV injection. Locomotor recovery in the AAV-fnD group ($n = 11$) is better than in AAV-GFP group ($n = 9$). Shown are mean values ± SEM. Asterisk indicates statistical significance (*t*-test) (*$P < 0.05$). AAV, adeno-associated virus; BMS, Basso Mouse Scale; fnD, fibronectin type III homologous domain D; GFP, green fluorescent protein.

caudal to the lesion site (86 ± 7.7 AU; **Figure 6d**). It is noteworthy that prominent TNC expression was visible in both gray and white matter of the spinal cord including the dorsal and the lateral funiculi occupied by the main descending axonal tracts, including the CST. Results of western blot analysis were consistent with the fluorescence intensity evaluation in that TNC is more expressed in the spinal cord rostral to the lesion site (1.96 ± 0.06 AU), less in the spinal cord caudal to the lesion site (1.34 ± 0.08 AU), and least in the intact spinal cord (0.95 ± 0.05 AU; **Figure 6c**). These observations, in conjunction observations of on injury-induced axonal retraction, suggest that TNC exerts a positive influence on the integrity of severed axonal stumps rostral to the lesion site.

Rescue of injury-induced axonal retraction in TNC$^{-/-}$ mice by exogenous TNC

To test the assumption that TNC is essential for maintenance of axonal integrity, we administered the TNC-derived fusion protein GST-fnD to the injured spinal cord of TNC$^{-/-}$ and TNC$^{+/+}$ mice. This fnD TNC promotes neurite outgrowth *in vitro* and is derived from TNC splice variants closely related to periods of increased axonal growth in the developing CNS.[14–16,20–22,36] In control TNC$^{-/-}$ mice, which received only GST, the distance between the lesion center and the tips of the CST axons was 1,160 ± 280 µm on average (see **Figure 7** for individual values), which is similar to the distance of retraction in lesioned and untreated TNC$^{-/-}$ mice (see earlier text). In TNC$^{-/-}$ mice treated with GST-fnD fusion protein, axonal retraction was significantly reduced to 446 ± 93 µm ($P < 0.05$, *t*-test, compared with control treatment). This result shows that the amount of GST-fnD that had been applied to the injured spinal cord of TNC$^{-/-}$ mice is sufficient to reduce the overt retraction to levels seen in TNC$^{+/+}$ mice. Exogenous TNC application to TNC$^{+/+}$ mice did not influence the extent of axonal retraction (axonal retraction of 304 ± 79 and 261 ± 48 µm in TNC$^{+/+}$ mice, which received GST-fnD fusion protein or glutathione *S*-transferase (GST) alone, respectively; no significant difference by *t*-test; see **Figure 7** for individual values). The experiment using fnD and GST proteins was designed to test effects on the integrity of corticospinal axons. To deliver maximum amounts of protein locally, a catheter was inserted in the subdural space at the level of cauda equina, passed along the sacral and lumbar spinal segments and its tip was fixed in close vicinity of the lesion scar. This positioning of the catheter caused, as indicated by histological examinations, some damage to the distal spinal cord that precluded use of outcome measures used for TNC$^{-/-}$ and TNC$^{+/+}$ mice like analyses of locomotion, H-reflex, and monaminergic axons.

AAV-fnD improves functional recovery in wild-type mice after spinal cord injury

Considering the negative effects of TNC deficiency on spinal cord regeneration and the rescue of injury-induced axonal retraction in TNC$^{-/-}$ mice by exogenous TNC, we tested the effect of a long-lasting viral-mediated delivery of TNC on functional recovery. We designed AAV vectors, which carry either the fnD-c-myc gene or the GFP gene for *in vivo* application.[6] We injected AAV-fnD ($n = 11$) or AAV-GFP ($n = 9$) into the spinal cords of TNC$^{+/+}$ mice immediately after injury and detected the expression of the target genes by staining the c-myc tagged on the fnD 1 week after the injection (**Supplementary Figure S1**). The expression lasted for at least 8 weeks after the injection, the longest observation time (data not shown). Analyses of locomotor recovery revealed a strong positive effect of AAV-fnD compared to AAV-GFP, which was apparent as early as 2 weeks after injury and lasted for the whole observation period of 8 weeks (**Figure 8**). The results of this experiment clearly indicate that TNC-fnD improves spinal cord regeneration and that its delivery by viral vectors to the injured spinal cord can be considered as a potential therapeutic approach.

© The American Society of Gene & Cell Therapy

AAV-fnD increases regrowth/sprouting of monaminergic axons and reduces lesion scar volume in wild-type mice

Because significant correlations had been found between functional recovery, evaluated by either foot-stepping angle or BMS score, and monaminergic reinnervation of the distal spinal cord after injury,[33] on one hand, and TNC deficiency reduced monaminergic regrowth/sprouting (**Figure 4**), on the other, we examined whether enhanced functional recovery in AAV-fnD-treated wild-type mice could be related to improved monaminergic reinnervation. Quantification of TH^+ axons in the distal spinal cords revealed that the numbers of monaminergic fibers at 8 weeks were significantly higher in AAV-fnD-treated mice (69 ± 11; n = 8) than in AAV-GFP-treated controls (28 ± 1.6; n = 7, $P < 0.01$). This observation indicates a more vigorous regenerative response of monaminergic fibers in the AAV-fnD-treated spinal cords. In contrast to TH^+ axons, anterograde labeling revealed that AAV-fnD in C57BL/6J mice, similar to GST-fnD in $TNC^{+/+}$ mice, did not attenuate the retraction of corticospinal axons (axonal retraction of 433 ± 23 and 480 ± 43 µm in AAV-fnD- and AAV-GFP-treated mice, n = 6 for each group, $P > 0.05$, t-test). This finding is not in contradiction to the observed functional effects since the locomotor abilities estimated by the BMS score and the foot stepping angle are not dependent on CST functions.[6]

Previous study also demonstrated a high degree of covariation between functional estimates and scar volume after spinal cord injury in mice.[6] We hence examined the lesion scar volume and observed that the volume was smaller in the AAV-fnD-treated mice (0.67 ± 0.08 mm^3; n = 8) compared with controls (1.03 ± 0.09 mm^3; n = 7, $P < 0.05$). This observation, taken together with the improved regrowth/sprouting of TH^+ axons in the AAV-fnD-treated spinal cords, indicates that AAV-fnD exerts its beneficial effects through decrease in scaring and improved axonal regeneration after spinal cord injury.

DISCUSSION

Here, we provide evidence that TNC is beneficial for CNS regeneration. $TNC^{-/-}$ mice show reduced locomotor recovery after spinal cord injury when compared with $TNC^{+/+}$ littermates. This inferior outcome is associated with attenuated H-reflex excitability and reduced survival and/or sprouting of axons. Positive functional effects were achieved by infusion of TNC-fnD into the spinal cord and overexpression of this TNC domain in the injured spinal cord of wild-type mice *via* a viral construct.

Mechanisms of TNC influence on spinal cord regeneration

Upregulation of TNC has previously been observed after lesions of the CNS,[10,13,37] but its role in tissue repair has not been understood. Our results indicate that TNC has beneficial functions after spinal cord lesion by preservation of axonal integrity and/or sprouting. In $TNC^{-/-}$ mice, myelinated corticospinal axons undergo a more pronounced secondary degeneration and nonmyelinated monaminergic axons distal to the site of injury are less numerous compared with $TNC^{+/+}$ mice. Moreover, administration of a beneficial domain of TNC, TNC-fnD, rescues this degeneration. These findings are in agreement with previous observations that TNC, when presented to growing neurites as a uniform substrate, enhances neurite outgrowth and supports neuronal survival.[14–17,36] In addition to influences exerted by TNC in close vicinity of axons, TNC may influence axonal survival by more indirect mechanisms.

In addition to neuroprotection, we have to consider that TNC is involved in synaptic plasticity.[21] The observed reduction of spinal afferent inputs to lamina VII in the spinal cords of injured $TNC^{-/-}$ mice may reflect a region-specific effect on injury-induced synaptic remodeling. In line with this notion is the finding that TNC overexpression is associated with seizure-induced synaptic formation in the hippocampus.[38] The positive effects of TNC on regeneration may not be restricted to the CNS: TNC expression is upregulated in various tissues after injury, for example, peripheral nerve, skin, and skeletal muscle[39,40] and the absence of TNC has negative impacts on the outcome of facial nerve injury.[41] Therefore, substantial evidence indicates that TNC promotes healing in various tissues.

Therapeutic potential of TNC

The scanty knowledge of the mechanisms regulating TNC expression in the injured spinal cord currently precludes the possibility to devise strategies for enhancement of its expression *via* regulatory pathways. Therefore, we used an AAV construct, previously shown to be an efficient vehicle for exogenous protein expression in the injured spinal cord,[42] to achieve overexpression of the neurite outgrowth-promoting fnD of TNC in wild-type, *i.e.*, TNC-competent, mice. Because AAV constructs are considered compatible with clinical applications,[43] the functional and morphological improvement observed in TNC-fnD-treated mice compared with control animals is promising. Moreover, it is conceivable that combinatorial AAV-based treatments using, in addition to TNC, other molecules beneficial for regeneration, such as L1,[42] or combination with treatment of regeneration conducive chondroitinase ABC, proteases, cytokines, and other agents could generate a higher potential for treatment of spinal cord injury and other CNS traumas and diseases. Simultaneous overexpression of TNC and TNC receptors may be another efficient approach. This notion is supported by recent observations that AAV-mediated overexpression of α9 integrin, a receptor for the nonalternatively spliced region of TNC, in DRG and spinal cord neurons in adult rats, increases regeneration of sensory axons and enables recovery of thermosensation.[44] Efficient delivery of TNC may not be restricted to viral constructs, as a neurite outgrowth-promoting peptide derived from the fnD of TNC also promotes axonal regeneration in the hemisected spinal cord of wild-type rats when covalently attached to polyamide nanofibers.[45]

MATERIALS AND METHODS

Animals. C57BL/6J mice (female, 8 weeks old) were purchased from Taconic (Hudson, NY). TNC-deficient mice were derived from the original stock.[24] Heterozygous ($TNC^{+/-}$) mice were intercrossed to yield homozygous TNC-deficient ($TNC^{-/-}$) and wild-type ($TNC^{+/+}$) littermates on a C57BL/6J genetic background after six generations of backcrossing with C57BL/6J mice. Genotypes were determined by PCR analysis using primers derived from the intron between exons 1 and 2 (5′-AGC CCC

© The American Society of Gene & Cell Therapy

TGC CTA CCT TTT CCT AAT G-3′), from the single *Lox*P–*Bam*HI site (5′-CCA GCT TTA TCG GAT CCA TAA CTT CG-3′), and from exon 2 (5′-CTT CGG GAG TGA GGG CAA ACA AAG-3′).

Antibodies. The polyclonal antibodies pK7 and KAF 9-2 to TNC have been described.[8] Rabbit polyclonal antibody to glial fibrillary acidic protein and mouse monoclonal antibody to fibronectin were purchased from Sigma Chemical (St Louis, MO). Rabbit polyclonal antibody to TH and mouse monoclonal antibody to glyceraldehyde-3-phosphate dehydrogenase (MAB374) were purchased from Chemicon (Hofheim, Germany). Mouse monoclonal antibody against VGLUT1 was purchased from Synaptic Systems (Göttingen, Germany). For indirect immunofluorescence and western blot analysis, secondary antibodies against rabbit or mouse IgGs and conjugated with Cy2, Cy3, or horseradish peroxidase were purchased from Dianova (Hamburg, Germany).

Spinal cord injury. All surgical procedures and postoperative care were approved by the local authorities and were in agreement with the guidelines of the European Community and the National Institutes of Health. The animals were deeply anesthetized by intraperitoneal injection (0.01 ml/g body weight) with a mixture of Ketanest (ketamine) (20%; Parke-Davis, Berlin, Germany) and Rompun (xylazine) (8%; Bayer, Leverkusen, Germany). Laminectomy was performed at the T7–T9 level with mouse laminectomy forceps (Fine Science Tools, Heidelberg, Germany). The spinal cord was compressed by a mouse spinal cord compression device.[42] This device controls a pair of watchmaker forceps, which are mounted on a metal block attached to a stereotaxic frame and automated with regard to the force and time of compression by an electromagnetic device. The spinal cord was compressed for 1 second by a time-controlled current flow through the electromagnetic drive. The skin was closed using 6-0 nylon sutures (Ethicon, Norderstedt, Germany). The operated mice were kept at 37 °C for 12 hours to prevent hypothermia. Afterward, they were housed individually in standard cages and kept in a conditioned room (22 °C) with standard water and food provided *ad libitum*. If animals died prior to the time points they were excluded from the cohort.

Evaluation of motor functions. The recovery of ground locomotion was evaluated using a mouse rating scale, the BMS.[26] In addition, motor recovery was analyzed using a numerical measure for plantar stepping evaluation, the foot-stepping angle.[6] In brief, a left- and a right-side view of each animal during two consecutive walking trials on a wooden beam (1-m long, 4-cm wide) was captured before the operation and at various time points after the operation with a video camera (A602fc camera; Basler, Ahrensburg, Germany) at 100 frames per second and analyzed with the affiliated analysis software (SIMI Motion; SIMI Reality Motion Systems, Unterschleissheim, Germany).

H-reflex recordings. Preparation of animals and the H-reflex recording technique were previously described.[27] Briefly, under ketamine–xylazine anesthesia (see earlier text), a ground needle electrode was applied at the base of the animal's tail. Needle electrodes (stainless steel, diameter: 0.4 mm) were used for sciatic nerve stimulation. The stimulating electrodes were inserted between the two heads of the biceps femoris muscle in the thigh so that the cathode was located rostrally to the anode. For electromyography recordings, a reference stainless steel electrode was fixed to the skin between the first and second digit and an active recording electrode (tungsten, diameter: 0.25 mm) was inserted between the second and the third cuneiform bones. Electrode positioning was performed under a stereomicroscope. The sciatic nerve was stimulated using bipolar electrical pulses of 0.2-ms duration to elicit reflex responses. Stimulus intensity was gradually increased until both M- and H-waves with latencies of ~2 and 5 ms, respectively, were visible. After the threshold measurement, stimulus intensity was further increased until maximal and stable H-responses were elicited. Thereafter, stimulation continued at the defined suprathreshold level at frequencies of 0.1, 0.3, 0.5, 1, 2, 3, and 5 Hz. Six consecutive responses were recorded at each frequency. The amplitudes of M- and H-waves were measured as peak-to-peak values, averaged (excluding the first response at each frequency) and used to calculate H/M ratios. The latencies of the responses were measured as time elapsed between trigger and peak of each waveform.

Anterograde labeling of CST. For CST anterograde labeling, $TNC^{+/+}$ and $TNC^{-/-}$ mice were subjected to the spinal cord injury according to the time points (7 days, 14 days and 30 days, for number of mice per group, see legend to **Figure 5**). Seven days before being perfused, the animals were anesthetized and their heads were fixed in a stereotaxic frame. Three 1-mm wide holes were drilled through the cranium overlying the sensorimotor cortex (coordinates: –0.5 mm, –1.75 mm, –3.0 mm Bregma, 2 mm lateral, 2 mm deep).[42] A glass micropipette was used to inject 2 µl of a 10% solution of fluoro-ruby (dextran tetramethylrhodamine 10,000 MW, lysine fixable; Molecular Probes, Eugene, OR) into the motor cortex. Animals survived for 7 days. Serial, 30-µm thick parasagittal sections were obtained from the spinal cords. The sections were analyzed by confocal microscopy. To quantify axon retraction,[34] the center of the compression lesion was chosen as a reference point. The distance between this point and the nearest detectable axon tips of the CST were measured.

Injection of TNC-fnD-GST fusion protein. To probe whether exogenous TNC can compensate for the loss of TNC in $TNC^{-/-}$ mice, TNC-derived fusion protein GST-fnD, which corresponds to the alternatively spliced fibronectin type III homologous repeat D of human TNC, and was previously shown to enhance neurite outgrowth *in vitro*,[22,36] was administered into the injured spinal cord locally by means of a catheter (300 µm outer diameter, 100 µm inner diameter) connected to an Alzet osmotic pump (Model 1002; DURECT, Cupertino, CA). The GST-fnD fusion protein was tested for bioactivity and found to be neurite outgrowth promoting *in vitro* in the presence of the GST tag (data not shown). The catheter was inserted in the subdural space at the level of cauda equina, passed along the sacral and lumbar spinal segments and its tip was fixed 2 mm caudal to the lesion site. FnD-GST (200 µg/ml, dissolved in 0.9% saline solution) was infused at a rate of 0.25 µl/hour for 14 days. Control animals were infused with GST. Anterograde labeling of the CST was introduced 23 days after spinal cord injury. Mice were euthanized 7 days after tracer injection, *i.e.*, 30 days after spinal cord injury.

AAV vector production. An AAV serotype 5–based viral vector was constructed to express the secreted form of TNC-fnD. The vector genome consisted of AAV-2 inverted terminal repeats, the short version (530 bp) of the murine immediate-early cytomegalovirus promoter, a C-terminally c-myc tagged complementary DNA encoding TNC-fnD (directed for secretion by an N-terminal fusion to the signal peptide of secreted alkaline phosphatase), the woodchuck hepatitis virus post-translational control element for enhanced transgene expression, and a bovine growth hormone polyadenylation site. This type of viral vector has been demonstrated to permit transgene expression in neurons and glial cells of the lesioned spinal cord.[42] Vectors were produced by transient transfection of HEK-293 cells using pDP5 as a helper plasmid. Cells were harvested at 2.5 days after transfection, viral particles were purified by iodixanol step-gradient centrifugation and fast protein liquid chromatography (Äkta FPLC; Amersham Biosciences, Freiburg, Germany) on 1 ml Q-FF anion-exchange column (GE Healthcare, Freiburg, Germany), dialysis against excess amounts of phosphate-buffered saline, and concentration on centrifugal spin concentrators (150 kd cutoff; Orbital Biosciences, Dulles, VA). Vector genomes were determined by quantitative PCR, and purity was confirmed to be at least 99.5% by sodium dodecyl sulfate–polyacrylamide gel electrophoresis and silver staining (data not shown).

AAV-TNC-fnD and AAV-GFP injection. The virus was injected into the lesion site immediately after compression spinal cord injury as described.[42] In brief, the viral constructs AAV-TNC-fnD and AAV-GFP (3×10^7 transducing units in 1 µl) were injected with a nanoliter microinjector

© The American Society of Gene & Cell Therapy

(World Precision Instruments, Sarasota, FL) over a time period of 5 minutes. The needle was kept in the tissue for another 2 minutes before it was slowly withdrawn.

Histological processing. Mice were anesthetized and perfused with 4% formaldehyde in 0.1 mol/l phosphate buffer, pH 7.4. The spinal cords were dissected and postfixed in the same fixative overnight at 4 °C. Spinal cords were embedded in Tissue-Tek (Sakura Finetek Europe, Zoeterwoude, The Netherlands) and frozen in isopentane precooled with liquid nitrogen. Spinal cords were then cut transversely or parasagittally on a cryostat to obtain serial 25-µm thick sections. Sections were collected on Superfrost Plus slides (Menzel, Braunschweig, Germany) from 25 equidistant (600-µm spaced) segments of the spinal cord, *i.e.*, up to 1.5 cm rostrally and caudally from the lesion epicenter. The lesion center was designated as level "L".

Immunohistochemistry. Sections were subjected to antigen retrieval in 10 mmol/l sodium citrate solution (80 °C, 30 minutes), followed by non-specific blocking with normal goat serum (room temperature, 1 hour) before the application of the primary antibodies. For counting TH^+ axons and $VGLUT1^+$ synaptic terminals, antibodies were used at optimal dilutions (1:800 and 1:500, respectively). For detection of TNC, fibronectin and glial fibrillary acidic protein, antibodies against TNC (1:500), fibronectin (1:500), and glial fibrillary acidic protein (1:500) were applied to the sections overnight at 4 °C followed by Cy2- or Cy3-conjugated anti-rabbit IgG antibodies. All sections were counterstained with bis-benzimide (Hoechst dye 32258) (Sigma Chemical) and, after washing, mounted with Aqua-Poly/mount (Polysciences, Warrington, PA). Sections were viewed on a fluorescence microscope (Axiophot 2, Zeiss, Thornwood, NY) and/or a confocal laser microscope (LSM 510, Zeiss). Gray value measurements were performed with ImageJ software (National Institute of Health, USA, free software available at http://rsb.info.nih.gov/ij/) from digital images.

Parasagittal spinal cord sections stained for TH were used to analyze monaminergic axons in the lumbar spinal cord. TH^+ axons projecting beyond an arbitrarily selected border 250 µm caudally to the lesion site were counted in every 5th parasagittal serial section from the spinal cord of each animal on an Axiophot 2 microscope (Zeiss) equipped with a motorized stage and Neurolucida software-controlled computer system (MicroBrightField Europe, Magdeburg, Germany).

To investigate densities of $VGLUT1^+$ synaptic terminals, transverse spinal cord sections caudal to the lesion scar were used for analysis. Digital images were obtained on an LSM 510 confocal microscope using a ×63 oil immersion objective and a digital resolution of 1,024 × 1,024 pixels. The gray value was adjusted using threshold to convert the images to gray scale for optimal color intensity with ImageJ software. Criteria for identification of synaptic terminals were: objects with size >2 µm^2 and circularity 0–1. Number and perimeter of synaptic terminals were sampled in the Clarke's column, lamina VII, and lamina IX (**Figure 3**) of each section. Density was calculated as number of $VGLUT1^+$ synaptic terminals per unit area. The values for left and right areas were averaged for each section. Six sections 250 µm apart were analyzed per animal, and the mean values from individual animals were used to calculate group mean values.

To estimate the lesion scar volume, spaced serial sections 250 µm apart were stained with fibronectin and used for estimations of the scar volume using the Cavalieri principle as described previously.[6] Areas of the scar required for volume estimation were measured by ImageJ software.

Western blot analysis. For western blot analysis, four $TNC^{+/+}$ and four $TNC^{-/-}$ mice were euthanized 4 days after spinal cord injury. The spinal cords were dissected out on ice and divided into two segments with regard to the lesion center, one rostral to the lesion center and the other caudal to it, with 5-mm length for each segment. The samples were then homogenized separately, centrifuged at 1,000 g and 4 °C for 15 minutes to remove insoluble material, and the supernatants were collected. Protein concentrations were determined by the bicinchoninic acid assay (Pierce Chemical, Rockford, IL). Samples were subjected to 8% sodium dodecyl sulfate–polyacrylamide gel electrophoresis and transferred onto a nitrocellulose membrane following standard protocols.[42] Signal was detected by an enhanced chemiluminescence detection system (Amersham Biosciences Europe, Freiburg, Germany). Equal amounts of protein were loaded into each lane and band intensities were normalized to those of glyceraldehyde-3-phosphate dehydrogenase.

Statistical analyses. Data were collected in a blinded manner. Group mean values were compared using two-sided Student's *t*-test for independent samples or one-way analysis of variance for repeated measurements and *post hoc* Tukey's test. The accepted level of significance was 5%. Values are shown as mean values with standard errors of the mean (SEM).

SUPPLEMENTARY MATERIAL

Figure S1. Expression of transgene products 1 week after spinal cord compression and injection of AAV-fnD or AAV-GFP.

ACKNOWLEDGMENTS

We are grateful to Fabio Morellini for breeding of $TNC^{+/+}$ and $TNC^{-/-}$ mice, Mirjam Sibbe for discussions, Emanuela Szpotowicz for technical assistance, Achim Dahlman for genotyping, Charles ffrench-Constant for comments on the manuscript, and the German Research Society (GRK 255, SPP 1109 and SPP 1135), Canadian Spinal Research Organization, The Daniel Heumann Fund for Spinal Cord Research and the National Institutes of Health (R01 NS40394) for support. M.S. is New Jersey Professor of Spinal Cord Research.

REFERENCES

1. GrandPré, T, Nakamura, F, Vartanian, T and Strittmatter, SM (2000). Identification of the Nogo inhibitor of axon regeneration as a Reticulon protein. *Nature* **403**: 439–444.
2. McKerracher, L, David, S, Jackson, DL, Kottis, V, Dunn, RJ and Braun, PE (1994). Identification of myelin-associated glycoprotein as a major myelin-derived inhibitor of neurite growth. *Neuron* **13**: 805–811.
3. Wang, KC, Koprivica, V, Kim, JA, Sivasankaran, R, Guo, Y, Neve, RL *et al.* (2002). Oligodendrocyte-myelin glycoprotein is a Nogo receptor ligand that inhibits neurite outgrowth. *Nature* **417**: 941–944.
4. Niclou, SP, Franssen, EH, Ehlert, EM, Taniguchi, M and Verhaagen, J (2003). Meningeal cell-derived semaphorin 3A inhibits neurite outgrowth. *Mol Cell Neurosci* **24**: 902–912.
5. Jones, LL, Margolis, RU and Tuszynski, MH (2003). The chondroitin sulfate proteoglycans neurocan, brevican, phosphacan, and versican are differentially regulated following spinal cord injury. *Exp Neurol* **182**: 399–411.
6. Apostolova, I, Irintchev, A and Schachner, M (2006). Tenascin-R restricts posttraumatic remodeling of motoneuron innervation and functional recovery after spinal cord injury in adult mice. *J Neurosci* **26**: 7849–7859.
7. Bradbury, EJ, Moon, LD, Popat, RJ, King, VR, Bennett, GS, Patel, PN *et al.* (2002). Chondroitinase ABC promotes functional recovery after spinal cord injury. *Nature* **416**: 636–640.
8. Bartsch, U, Faissner, A, Trotter, J, Dörries, U, Bartsch, S, Mohajeri, H *et al.* (1994). Tenascin demarcates the boundary between the myelinated and nonmyelinated part of retinal ganglion cell axons in the developing and adult mouse. *J Neurosci* **14**: 4756–4768.
9. Steindler, DA, Settles, D, Erickson, HP, Laywell, ED, Yoshiki, A, Faissner, A *et al.* (1995). Tenascin knockout mice: barrels, boundary molecules, and glial scars. *J Neurosci* **15**: 1971–1983.
10. Zhang, Y, Winterbottom, JK, Schachner, M, Lieberman, AR and Anderson, PN (1997). Tenascin-C expression and axonal sprouting following injury to the spinal dorsal columns in the adult rat. *J Neurosci Res* **49**: 433–450.
11. Jones, FS and Jones, PL (2000). The tenascin family of ECM glycoproteins: structure, function, and regulation during embryonic development and tissue remodeling. *Dev Dyn* **218**: 235–259.
12. Nakic, M, Manahan-Vaughan, D, Reymann, KG and Schachner, M (1998). Long-term potentiation *in vivo* increases rat hippocampal tenascin-C expression. *J Neurobiol* **37**: 393–404.
13. Nakic, M, Mitrovic, N, Sperk, G and Schachner, M (1996). Kainic acid activates transient expression of tenascin-C in the adult rat hippocampus. *J Neurosci Res* **44**: 355–362.
14. Husmann, K, Faissner, A and Schachner, M (1992). Tenascin promotes cerebellar granule cell migration and neurite outgrowth by different domains in the fibronectin type III repeats. *J Cell Biol* **116**: 1475–1486.
15. Lochter, A and Schachner, M (1993). Tenascin and extracellular matrix glycoproteins: from promotion to polarization of neurite growth *in vitro*. *J Neurosci* **13**: 3986–4000.
16. Dörries, U, Taylor, J, Xiao, Z, Lochter, A, Montag, D and Schachner, M (1996). Distinct effects of recombinant tenascin-C domains on neuronal cell adhesion, growth cone guidance, and neuronal polarity. *J Neurosci Res* **43**: 420–438.

© The American Society of Gene & Cell Therapy

17. Taylor, J, Pesheva, P and Schachner, M (1993). Influence of janusin and tenascin on growth cone behavior *in vitro*. *J Neurosci Res* **35**: 347–362.
18. Meiners, S and Geller, HM (1997). Long and short splice variants of human tenascin differentially regulate neurite outgrowth. *Mol Cell Neurosci* **10**: 100–116.
19. Meiners, S, Mercado, ML, Nur-e-Kamal, MS and Geller, HM (1999). Tenascin-C contains domains that independently regulate neurite outgrowth and neurite guidance. *J Neurosci* **19**: 8443–8453.
20. Rigato, F, Garwood, J, Calco, V, Heck, N, Faivre-Sarrailh, C and Faissner, A (2002). Tenascin-C promotes neurite outgrowth of embryonic hippocampal neurons through the alternatively spliced fibronectin type III BD domains via activation of the cell adhesion molecule F3/contactin. *J Neurosci* **22**: 6596–6609.
21. Dityatev, A and Schachner, M (2003). Extracellular matrix molecules and synaptic plasticity. *Nat Rev Neurosci* **4**: 456–468.
22. Mercado, ML, Nur-e-Kamal, A, Liu, HY, Gross, SR, Movahed, R and Meiners, S (2004). Neurite outgrowth by the alternatively spliced region of human tenascin-C is mediated by neuronal α7β1 integrin. *J Neurosci* **24**: 238–247.
23. Liu, HY, Nur-E-Kamal, A, Schachner, M and Meiners, S (2005). Neurite guidance by the FnC repeat of human tenascin-C: neurite attraction vs. neurite retention. *Eur J Neurosci* **22**: 1863–1872.
24. Evers, MR, Salmen, B, Bukalo, O, Rollenhagen, A, Bösl, MR, Morellini, F *et al.* (2002). Impairment of L-type Ca^{2+} channel-dependent forms of hippocampal synaptic plasticity in mice deficient in the extracellular matrix glycoprotein tenascin-C. *J Neurosci* **22**: 7177–7194.
25. Basso, DM, Fisher, LC, Anderson, AJ, Jakeman, LB, McTigue, DM and Popovich, PG (2006). Basso Mouse Scale for locomotion detects differences in recovery after spinal cord injury in five common mouse strains. *J Neurotrauma* **23**: 635–659.
26. Morellini, F and Schachner, M (2006). Enhanced novelty-induced activity, reduced anxiety, delayed resynchronization to daylight reversal and weaker muscle strength in tenascin-C-deficient mice. *Eur J Neurosci* **23**: 1255–1268.
27. Lee, HJ, Jakovcevski, I, Radonjic, N, Hoelters, L, Schachner, M and Irintchev, A (2009). Better functional outcome of spinal cord injury in mice is associated with enhanced H-reflex excitability. *Exp Neurol* **513**: 496–510.
28. Lavrov, I, Dy, CJ, Fong, AJ, Gerasimenko, Y, Courtine, G, Zhong, H *et al.* (2008). Epidural stimulation induced modulation of spinal locomotor networks in adult spinal rats. *J Neurosci* **28**: 6022–6029.
29. Brumovsky, P, Watanabe, M and Hökfelt, T (2007). Expression of the vesicular glutamate transporters-1 and -2 in adult mouse dorsal root ganglia and spinal cord and their regulation by nerve injury. *Neuroscience* **147**: 469–490.
30. Erschbamer, M, Pernold, K and Olson, L (2007). Inhibiting epidermal growth factor receptor improves structural, locomotor, sensory, and bladder recovery from experimental spinal cord injury. *J Neurosci* **27**: 6428–6435.
31. Edgerton, VR, Tillakaratne, NJ, Bigbee, AJ, de Leon, RD and Roy, RR (2004). Plasticity of the spinal neural circuitry after injury. *Annu Rev Neurosci* **27**: 145–167.
32. Fouad, K and Pearson, K (2004). Restoring walking after spinal cord injury. *Prog Neurobiol* **73**: 107–126.
33. Jakovcevski, I, Wu, J, Karl, N, Leshchyns'ka, I, Sytnyk, V, Chen, J *et al.* (2007). Glial scar expression of CHL1, the close homolog of the adhesion molecule L1, limits recovery after spinal cord injury. *J Neurosci* **27**: 7222–7233.
34. Houle, JD and Jin, Y (2001). Chronically injured supraspinal neurons exhibit only modest axonal dieback in response to a cervical hemisection lesion. *Exp Neurol* **169**: 208–217.
35. Bareyre, FM, Kerschensteiner, M, Misgeld, T and Sanes, JR (2005). Transgenic labeling of the corticospinal tract for monitoring axonal responses to spinal cord injury. *Nat Med* **11**: 1355–1360.
36. Meiners, S, Nur-e-Kamal, MS and Mercado, ML (2001). Identification of a neurite outgrowth-promoting motif within the alternatively spliced region of human tenascin-C. *J Neurosci* **21**: 7215–7225.
37. Laywell, ED, Dörries, U, Bartsch, U, Faissner, A, Schachner, M and Steindler, DA (1992). Enhanced expression of the developmentally regulated extracellular matrix molecule tenascin following adult brain injury. *Proc Natl Acad Sci USA* **89**: 2634–2638.
38. Represa, A and Ben-Ari, Y (1997). Molecular and cellular cascades in seizure-induced neosynapse formation. *Adv Neurol* **72**: 25–34.
39. Daniloff, JK, Crossin, KL, Pinçon-Raymond, M, Murawsky, M, Rieger, F and Edelman, GM (1989). Expression of cytotactin in the normal and regenerating neuromuscular system. *J Cell Biol* **108**: 625–635.
40. Irintchev, A, Salvini, TF, Faissner, A and Wernig, A (1993). Differential expression of tenascin after denervation, damage or paralysis of mouse soleus muscle. *J Neurocytol* **22**: 955–965.
41. Guntinas-Lichius, O, Angelov, DN, Morellini, F, Lenzen, M, Skouras, E, Schachner, M *et al.* (2005). Opposite impacts of tenascin-C and tenascin-R deficiency in mice on the functional outcome of facial nerve repair. *Eur J Neurosci* **22**: 2171–2179.
42. Chen, J, Wu, J, Apostolova, I, Skup, M, Irintchev, A, Kügler, S *et al.* (2007). Adeno-associated virus-mediated L1 expression promotes functional recovery after spinal cord injury. *Brain* **130**: 954–969.
43. Perabo, L, Huber, A, Märsch, S, Hallek, M and Büning, H (2008). Artificial evolution with adeno-associated viral libraries. *Comb Chem High Throughput Screen* **11**: 118–126.
44. Andrews, MR, Czvitkovich, S, Dassie, E, Vogelaar, CF, Faissner, A, Blits, B *et al.* (2009). α9 Integrin promotes neurite outgrowth on tenascin-C and enhances sensory axon regeneration. *J Neurosci* **29**: 5546–5557.
45. Meiners, S, Ahmed, I, Ponery, AS, Amor, N, Harris, SL, Ayres, V *et al.* (2007). Engineering electrospun nanofibers for spinal cord repair: a discussion. *Polym Int* **56**: 1340–1348.